© 2017. Published by The Company of Biologists Ltd | Development (2017) 144, 400-408 doi:10.1242/dev.143958

Stage- and subunit-specific functions of polycomb repressive complex 2 in bladder urothelial formation and regeneration

Chunming Guo[1,*], Zarine R. Balsara[1,*], Warren G. Hill[2] and Xue Li[1,‡]

ABSTRACT

Urothelium is the protective lining of the urinary tract. The mechanisms underlying urothelial formation and maintenance are largely unknown. Here, we report the stage-specific roles of PRC2 epigenetic regulators in embryonic and adult urothelial progenitors. Without *Eed*, the obligatory subunit of PRC2, embryonic urothelial progenitors demonstrate reduced proliferation with concomitant dysregulation of genes including *Cdkn2a* (*p16*), *Cdkn2b* (*p15*) and *Shh*. These mutants display premature differentiation of keratin 5-positive (Krt5$^+$) basal cells and ectopic expression of squamous-like differentiation markers. Deletion of *Ezh2*, the major enzymatic component of PRC2, causes upregulation of *Upk3a*$^+$ superficial cells. Unexpectedly, *Eed* and *Eed*/*Ezh2* double mutants exhibit delayed superficial cell differentiation. Furthermore, *Eed* regulates the proliferative and regenerative capacity of adult urothelial progenitors and prevents precocious differentiation. Collectively, these findings uncover the epigenetic mechanism by which PRC2 controls urothelial progenitor cell fate and the timing of differentiation, and further suggest an epigenetic basis of urothelial maintenance and regeneration.

KEY WORDS: Mouse, Urothelium, Squamous differentiation, Bladder, Regeneration, Injury, Epigenetics, PRC2, Shh, Ezh2, Eed, Krt5, Krt14, Krt17

INTRODUCTION

The urinary bladder is an anterior extension of the urogenital sinus, the ventral region of the cloaca or the embryonic hindgut (Huang et al., 2016). Unlike gut epithelium, mature bladder urothelium is essentially quiescent with a low turnover rate (Jost, 1989). In response to injury, however, urothelium readily switches to a proliferative and regenerative mode to repair the damaged site. The mechanisms underlying urothelium formation and regeneration remain poorly understood.

Definitive bladder urothelium consists of three major cell types, keratin 5-positive (Krt5$^+$) basal cells, Krt20$^+$ superficial or umbrella cells, and Krt5- and Krt20-double negative intermediate cells (Georgas et al., 2015). Basal and intermediate cells represent ∼68% and ∼29%, respectively, of the entire population of mature bladder urothelium in adult mice (Jost, 1989). Superficial cells, which face directly to bladder lumen, are terminally differentiated large polyploid cells consisting of less than 3% of adult urothelium. During the early stages of bladder organogenesis between embryonic days (E)9.5 to E13.5 of murine embryos (Huang et al., 2016), the primitive bladder and gut epithelia originate from embryonic hindgut, as known as the cloaca, and share several common molecular signatures, including *Shh*, *Trp63* and *Foxa2*. Expression of uroplakin 1b (*Upk1b*) at the ventral subdomain of the cloaca marks the initial sign of bladder urothelial specification. These cells are the proposed P-cells (Gandhi et al., 2013). *Krt5* expression is detected much later at E15.0. Ectopic expression of *RaraDN*, the dominant negative form of retinoic acid (RA) receptor α, in P-cells results in the persistent expression of *Foxa2* and loss of intermediate and superficial cells (Gandhi et al., 2013). Conversely, RA treatment of cultured embryonic stem cells induces expression of uroplakin genes (Mauney et al., 2010), suggesting that the RA signaling pathway directs urothelial specification, particularly formation of the Upk$^+$ intermediate and superficial cell lineages.

Mature bladder urothelium has a very low turnover rate. However, injuries such as urinary tract infection (UTI) or cyclophosphamide (CPP) treatment trigger a rapid proliferative response of the basal and intermediate cells to regenerate superficial cells (Colopy et al., 2014; Gandhi et al., 2013; Kunze et al., 1980; Mysorekar et al., 2009; Papafotiou et al., 2016; Shin et al., 2011). While the molecular mechanisms underlying the urothelial quiescent state and regenerative capacity remain largely unknown, these studies begin to uncover the cellular basis of urothelial regeneration. *Shh* is expressed in primitive urothelial cells, P-cells and adult urothelium. Beachy and colleagues suggest that adult *Shh* expression is restricted to Krt5$^+$ basal cells (Shin et al., 2011). However, Mendelsohn and colleagues show that *Shh* is expressed in both basal and intermediate cell layers (Gandhi et al., 2013). Using *Shh*^{CreER}, a *Cre-ERT2* fusion gene inserted into the *Shh* genetic locus, to indelibly label *Shh*$^+$ progenitors and their daughter cells, both groups demonstrated that the genetically labeled *Shh*$^+$ cells proliferate and differentiate into superficial cells during urothelial injury and repair, indicating that *Shh*$^+$ cells function as adult urothelial progenitors (Gandhi et al., 2013; Shin et al., 2011). When Krt5$^+$ basal cells were indelibly labeled using a Cre transgenic line (Indra et al., 1999), no labeled cells were detected in the superficial cell layer after CPP treatment (Gandhi et al., 2013). *Krt14* marks a small subpopulation of Krt5$^+$ basal cells. Surprisingly, Krt14$^+$ cells contribute extensively to superficial cells after repeated CPP-induced bladder injury (Papafotiou et al., 2016). By comparing the urothelial response to different types of injuries, Mysorekar et al. (2009) noted that UTI and protamine sulfate preferentially induced basal and intermediate cell proliferation, respectively, suggesting that the cellular basis of urothelial regeneration may differ depending on the type and/or severity of injury. Collectively, mature urothelial cells are largely quiescent, but both basal and intermediate cells maintain proliferative potential and possible regenerative capacity.

[1]Department of Urology and Department of Surgery, Boston Children's Hospital, Harvard Medical School, 300 Longwood Avenue, Boston, MA 02115, USA. [2]Laboratory of Voiding Dysfunction, Department of Medicine, Beth Israel Deaconess Medical Center and Harvard Medical School, Boston, MA 02115, USA.
*These authors contributed equally to this work

‡Author for correspondence (sean.li@childrens.harvard.edu)

W.G.H., 0000-0002-2772-7264; X.L., 0000-0002-3072-0573

Received 22 August 2016; Accepted 12 December 2016

Development (2017) 144, 400-408 doi:10.1242/dev.143958

By regulating the chromatin state, epigenetic mechanisms are central to the establishment and maintenance of gene expression patterns in progenitors and differentiated cells (Margueron and Reinberg, 2011). The polycomb repressive complex 2 (PRC2) is responsible for trimethylation of histone H3 lysine 27 (H3K27me3), which is associated with transcription silencing (Cao et al., 2002; Czermin et al., 2002; Kuzmichev et al., 2002; Müller et al., 2002). Here, we used Cre/loxP technology to conditionally inactivate *Eed* and *Ezh2*, which encode the obligatory structural component (Montgomery et al., 2005) and the catalytic subunit of PRC2 (Cao et al., 2002; Kuzmichev et al., 2002), respectively, in embryonic or adult urothelial progenitors. Deletion of *Eed* but not *Ezh2* from embryonic urothelial progenitors caused premature differentiation of Krt5^{+} basal cells and ectopic expression of squamous cell markers. Deletion of *Eed* from adult urothelial progenitors resulted in precocious superficial cell differentiation and reduced regenerative capacity. Collectively, our findings demonstrate the stage- and subunit-specific roles of PRC2 epigenetic regulators in bladder urothelial progenitors during development and further suggest the epigenetic basis of urothelial regeneration after injury.

RESULTS

PRC2 activity is enriched in bladder urothelium

We analyzed H3K27me3 distribution to determine tissue-specific PRC2 activity in both embryonic and adult murine bladders. Strong H3K27me3 staining was detected in the urothelium with reduced expression in the lamina propria (LP) or smooth muscle cell (SMC) layers (Fig. 1A and Fig. S1A,B). Variable levels of H3K27me3 were observed among urothelial cells within the Krt5^{+} basal as well as Krt5^{-} intermediate and superficial cells (Fig. 1B). Expression of key PRC2 complex genes was further analyzed using microdissected bladder tissues. *Eed* expression was distributed uniformly within the urothelium and smooth muscle tissue at both adult and embryonic stages (Fig. 1C,D). In contrast, *Ezh2* was significantly enriched in the urothelium (Fig. 1C), with higher *Ezh2* expression in embryonic urothelium than adult urothelium (Fig. 1D). To study the role of the PRC2-dependent epigenetic program in the urothelium, *Eed* was conditionally deleted from embryonic urothelial progenitors by crossing a *Shh*^{GC} Cre driver, which expresses *eGFP* and *Cre* fusion gene (GC) in the primitive urothelium at E9.5 (Harfe et al., 2004; Seifert et al., 2008), with a conditional floxed allele of *Eed*$^{f/f}$ (Xie et al., 2014). The resulting

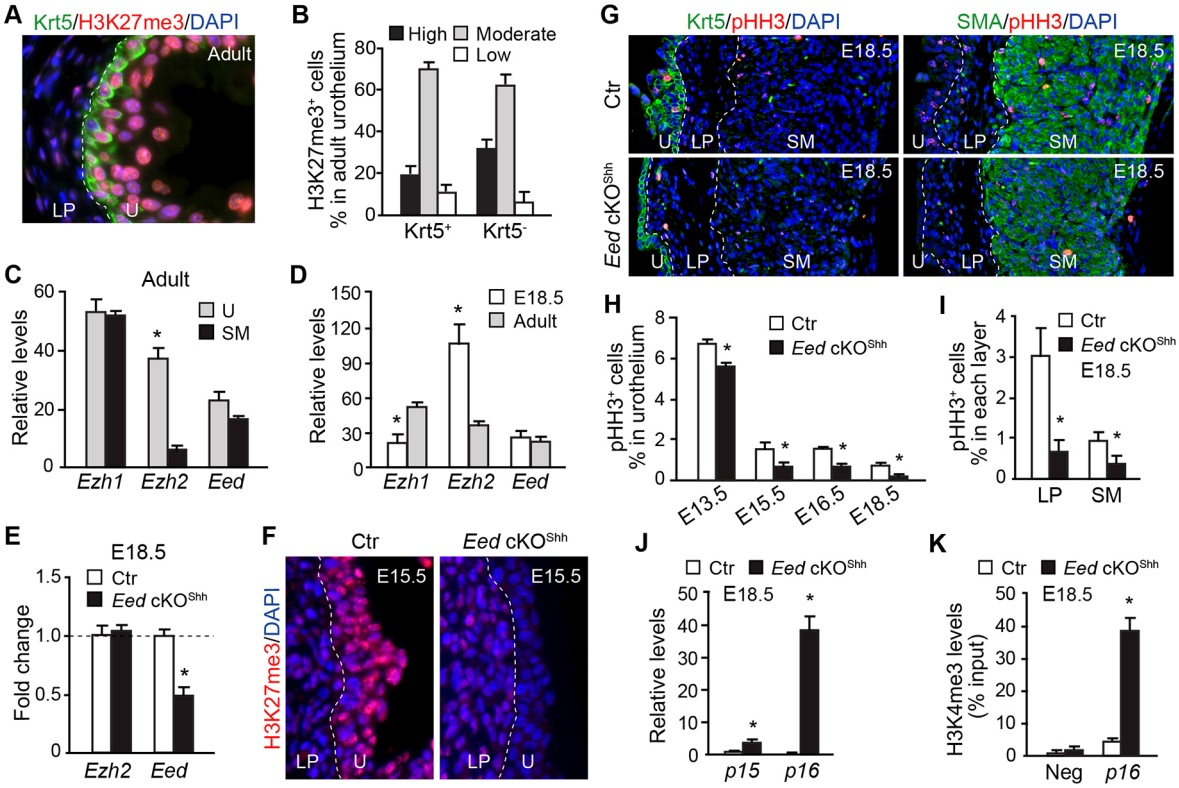

Fig. 1. Urothelium-specific PRC2 activity regulates bladder cell proliferation during development. (A) Immunofluorescence microscopy of bladder sections from P45 wild-type mice stained with Krt5 (green), H3K27me3 (red) and DAPI (blue). (B) Quantification of the relative levels of H3K27me3 expression in Krt5^{+} and Krt5^{-} urothelial cells. (C,D) qRT-PCR analysis of *Ezh1*, *Ezh2* and *Eed* expression relative to *Gapdh* in bladder urothelium (U) and smooth muscle (SM) at P45 (C) and urothelium of E18.5 and P45 bladders (D). (E) qRT-PCR analysis of control (Ctr) and *Eed* cKO^{Shh} microdissected urothelium at E18.5. (F) Immunofluorescence microscopy of bladder sections from E18.5 control and *Eed* cKO^{Shh} mice stained with H3K27me3 (red) and DAPI (blue). (G) Immunofluorescence microscopy of sections from E18.5 control and *Eed* cKO^{Shh} bladders stained with Krt5 (green, left), SMA (green, right), pHH3 (red) and DAPI (blue). (H) The percentage of pHH3^{+} cells within the urothelium was calculated relative to the total number of urothelial cells in control versus *Eed* cKO^{Shh} bladders from E13.5, E15.5, E16.5 and E18.5 embryos. Control (Ctr), *Eed*$^{fl/+}$;*Shh*$^{GC/+}$. (I) The percentage of pHH3^{+} cells within the lamina propria (LP) and smooth muscle (SM) was calculated relative to the total number of cells in each layer in E18.5 control versus *Eed* cKO^{Shh} bladders. (J) qRT-PCR analysis of *Cdkn2b* (*p15*) and *Cdkn2a* (*p16*) expression relative to *Gapdh* in microdissected urothelium from E18.5 control versus *Eed* cKO^{Shh} embryos. (K) ChIP-qPCR for H3K4me3 occupancy of the *p16* promoter versus an unrelated promoter (Neg) in control versus *Eed* cKO^{Shh} urothelium at E18.5. White dashed lines demarcate the different layers within the bladder. U, urothelium; LP, lamina propria; SM, smooth muscle. Data in C-E and H-K represent mean±s.e.m. of *n*=3-6. Unpaired Student's *t*-test, **P*<0.05.

Development (2017) 144, 400-408 doi:10.1242/dev.143958

urothelium-specific *Eed* conditional knockout embryos, namely *Eed* cKO^{Shh} (*Eed$^{f/f}$;Shh$^{GC/+}$*), exhibited a significant reduction in *Eed* transcripts from microdissected urothelium compared with compound heterozygous controls (*Eed$^{f/+}$;Shh$^{GC/+}$*) (Fig. 1E). More importantly, *Eed* cKO^{Shh} mice lacked any detectable H3K27me3 in the urothelium (Fig. 1F), confirming the central role of *Eed* in establishing the PRC2-dependent epigenetic program *in vivo*.

Urothelium-specific PRC2 has both cell-autonomous and non-autonomous functions

All *Eed* cKO^{Shh} mutants died shortly after birth, most likely because of a hypoplastic lung defect (Galvis et al., 2015; Snitow et al., 2015) (Fig. S2A,E,F). The lower urinary tract was grossly normal in these mutants (Fig. S2B). Histological analyses, however, demonstrated that the mutant urothelium was thinner (Fig. S2C,D). There was no detectable difference in levels of apoptosis at all stages analyzed (data not shown). However, cell proliferation rate as revealed by the mitotic marker phospho-histone H3 (pHH3) was significantly reduced in *Eed* cKO^{Shh} urothelium at all stages analyzed (Fig. 1G,H, E13.5-E18.5). Consistent with the urothelial proliferation defect, the canonical PRC2 target genes, including the cyclin-dependent kinase inhibitors 2A [*Cdkn2a* (*p16*)] and 2B [*Cdkn2b* (*p15*)] were significantly increased in the mutants (Fig. 1J). Concomitantly, the H3K4me3 epigenetic mark, which associates with active transcription, was significantly enriched at the *Cdkn2a* promoter region in the mutant urothelium (Fig. 1K). Unexpectedly, cell proliferation rates were also reduced in the LP and SM layers, indicating that the defect was not restricted to the urothelium (Fig. 1I). Expression of several smooth muscle differentiation genes was also upregulated (Fig. S3). Since *Eed* deletion is restricted to the urothelium, these findings collectively suggest that the PRC2-dependent urothelial epigenetic program has both cell-autonomous and non-autonomous functions during bladder development.

PRC2 regulates *Shh* expression in urothelial progenitors

The cell non-autonomous *Eed* activity probably depends upon downstream signaling molecules. To identify potential candidates, we focused on *Shh* because its activity is crucial for proliferation of the surrounding mesenchyme and differentiation of smooth muscle cells (DeSouza et al., 2013; Shin et al., 2011; Shiroyanagi et al., 2007). *Shh* and its receptors *Ptch1* and *Ptch2* were significantly reduced in *Eed* cKO^{Shh} mutant bladders compared with expression in bladders of littermate controls (Fig. 2A). Whole-mount RNA *in situ* hybridization demonstrated that *Shh* expression in bladder urothelium and the urethral groove of the genital tubercle was markedly reduced in the mutants (Fig. 2B). *Shh* expression in the preputial glands (PGs) was comparable between the mutants and controls, suggesting that PRC2 regulates *Shh* gene expression in a tissue-specific manner.

To understand how PRC2 may regulate *Shh*, we tested the hypothesis that PRC2 inhibited expression of transcriptional repressors, which negatively regulate *Shh* gene expression. *Pax6* is a known transcriptional repressor that directly inhibits expression of *Shh in vivo* (Caballero et al., 2014). *Pax6* is ectopically expressed in cardiomyocytes with deleted PRC2 (Delgado-Olguín et al., 2012; He et al., 2012). *Pax6* was undetectable in wild-type mouse bladders. However, high levels of *Pax6* were observed in mutant bladders at E15.5 and E18.5 based on both RNA *in situ* hybridization and quantitative RT-PCR analyses, respectively (Fig. 2C,D). Furthermore, ChIP analysis demonstrated that *Ezh2* was strongly associated with the promoter regions of *Pax6* in control urothelium, and *Ezh2* occupancy was significantly reduced in *Eed* cKO^{Shh} mutant urothelium (Fig. 2E). Conversely, the active epigenetic mark H3K4me3 was significantly elevated in mutant urothelium (Fig. 2F). These findings suggest that PRC2 indirectly promotes *Shh* expression via repression of genes, including *Pax6*, in fetal mouse bladder urothelium.

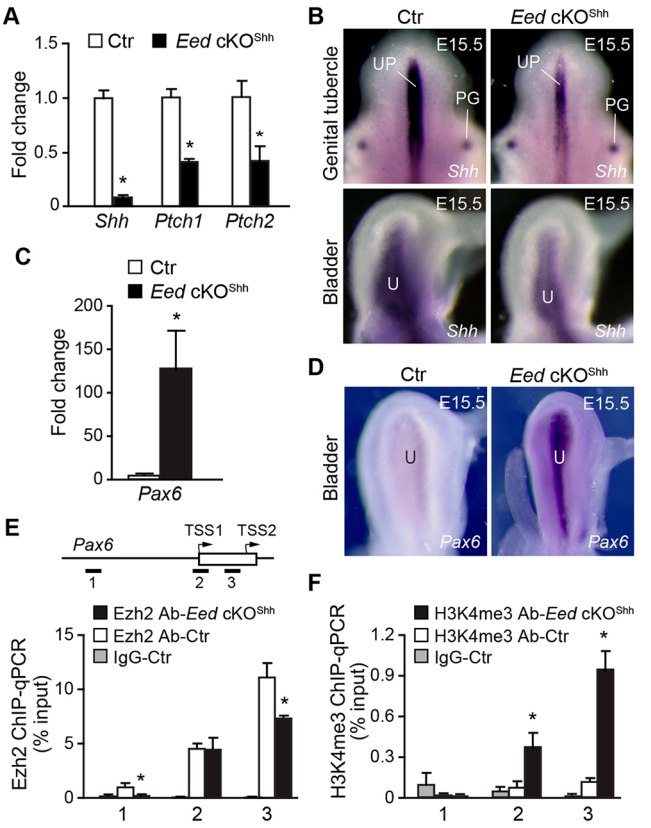

Fig. 2. Deletion of *Eed* results in downregulation of *Shh* in the developing urothelium. (A,C) qRT-PCR analysis of *Shh*, *Ptch1*, *Ptch2* and *Pax6* expression relative to *Gapdh* in whole bladders from E18.5 control (Ctr, *Eed$^{f/+}$;Shh$^{GC/+}$*) and *Eed* cKO^{Shh} embryos. Control transcript levels were normalized to 1.0 and transcript levels in *Eed* cKO^{Shh} samples are displayed as fold change relative to control. (B,D) Whole mount *in situ* hybridization of control (Ctr, *Eed$^{f/+}$;Shh$^{GC/+}$*) and *Eed* cKO^{Shh} mutants at E15.5 using RNA probes for *Shh* (B) and *Pax6* (D). PG, preputial glands; UP, urethral plate; U, urothelium. (E,F) ChIP-qPCR of *Pax6* locus using anti-Ezh2 (E) and anti-H3K4me3 (F) antibodies. Schematic in E indicates location of PCR oligos (1-3) and transcription start sites (TSS) of *Pax6*. Open box, exon; arrows, direction of transcription. Data in A,C,E,F represent mean±s.e.m. of *n*=3-6. Unpaired Student's *t*-test, **P*<0.05.

PRC2 regulates the timing of urothelial differentiation

Urothelial differentiation was analyzed using known cell type-specific molecular markers. Expression of uroplakin 3a (*Upk3a*), a superficial cell marker, was readily detected in wild-type bladders at E15.5 (Fig. 3A). In contrast, the basal cell marker Krt5 was barely detectable at this same stage. In *Eed* cKO^{Shh} mutants, *Upk3a* expression was reduced, with fewer Upk3a^{+} cells (Fig. 3A and Fig. S4A). In contrast, a large number of Krt5^{+} basal cells were observed in the mutant urothelium (Fig. 3A and Fig. S4B). Additionally, ectopic Krt5 expression was observed occasionally in Upk3a^{+} superficial cells (Fig. 3B, arrowheads). Nevertheless, by E16.5, expression levels of *Krt5* and *Upk3a* become comparable between the mutants and littermate controls. Thus, the PRC2-dependent epigenetic program regulates the timing of urothelial

Development (2017) 144, 400-408 doi:10.1242/dev.143958

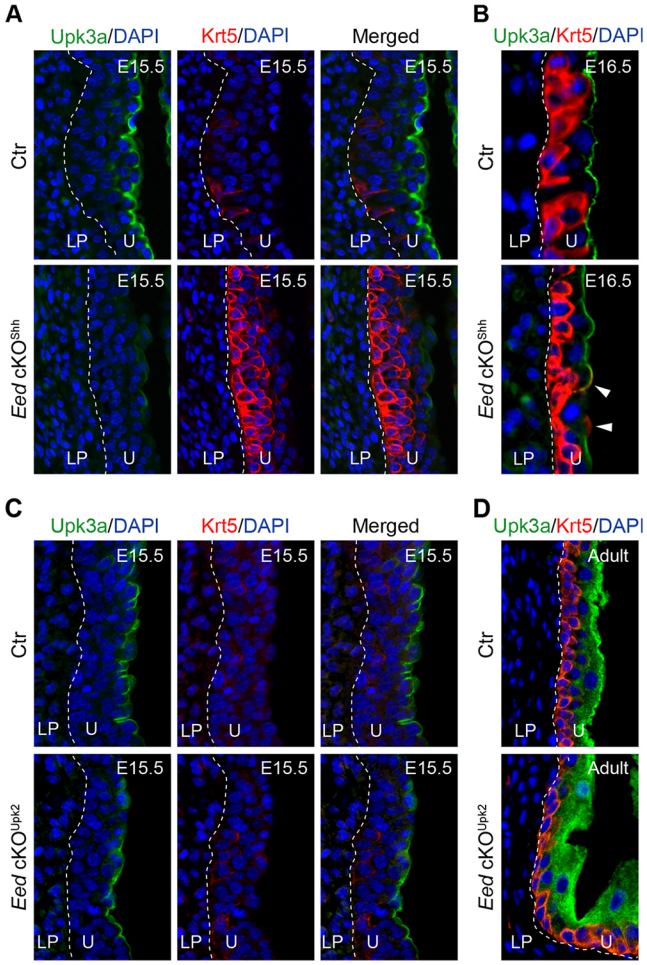

Fig. 3. Deletion of *Eed* from embryonic urothelial progenitors leads to premature differentiation of Krt5^{+} basal cells and delayed formation of Upk3a^{+} superficial cells. Immunofluorescence microscopy of bladder sections stained for Upk3a (green), Krt5 (red) and DAPI (blue). (A,B) control (Ctr, *Eed*$^{fl/+}$;*Shh*$^{GC/+}$) and *Eed* cKO^{Shh} bladder sections from E15.5 (A) and E16.5 (B) embryos. (C,D) Control (Ctr, *Eed*$^{fl/+}$;*Upk2-Cre*) and *Eed* cKO^{Upk2} (*Eed*$^{fl/f}$;*Upk2-Cre*) bladder sections from E15.5 (C) and adult (D) mice. White dashed lines demarcate the different layers within the bladder. Arrowheads indicate superficial cells that express both *Upk3a* and *Krt5*. U, urothelium; LP, lamina propria.

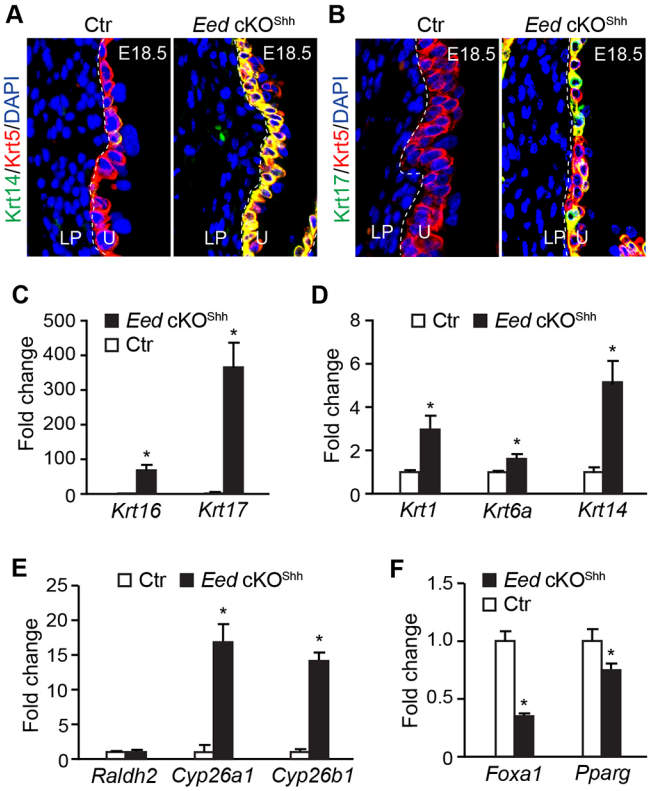

Fig. 4. Aberrant squamous-like differentiation of *Eed* cKO^{shh} mutant urothelium. (A) Immunofluorescence staining of bladder sections using antibodies against Krt5 (red) and Krt14 (green). Control (Ctr), *Eed*$^{fl/+}$;*Shh*$^{GC/+}$. (B) Immunofluorescence staining for Krt5 (red) and Krt17 (green). Blue, DAPI counter staining. (C-F) qRT-PCR analysis of gene expression levels relative to *Gapdh* in microdissected bladder urothelium from E18.5 control (Ctr, *Eed*$^{fl/+}$;*Shh*$^{GC/+}$) and *Eed* cKO^{Shh} embryos. Control transcript levels were normalized to 1.0 and transcript levels in *Eed* cKO samples are displayed as fold change relative to control. Data represent mean±s.e.m. of n=6. Unpaired Student's t-test, *P<0.05.

differentiation by attenuating basal cell formation while promoting superficial cell differentiation.

To examine whether PRC2 regulates *Krt5* and *Upk3a* gene expression and urothelial differentiation in a stage-specific manner, we deleted *Eed* from bladder urothelium starting at E13.5 (Fig. S5), using an *Upk2-Cre* driver (Kanasaki et al., 2013). As expected, overall levels of H3K27me3 were reduced in the urothelium of *UpkII-Cre*-mediated *Eed* conditional mutants, *Eed* cKO^{Upk2} (Fig. S6A). Cell proliferation rates were also significantly reduced in the *Eed* cKO^{Upk2} mutants (Fig. S6C,D). Despite these observations, the time course of basal and superficial cell differentiation in *Eed* cKO^{Upk2} mutants was comparable to wild-type littermate controls (Fig. 3C). Likewise, there was no apparent histological defect of the adult mutants (Fig. 3D, Fig. S6B). Collectively, these findings suggest a stage-specific role of PRC2 in controlling the timing of urothelial progenitor cell differentiation. Specifically, early Eed activity (from E9.5 and on) in primitive urothelium and P-cells is crucial for urothelial cell proliferation and differentiation. However, late Eed activity (after E13.5) in intermediate and basal cells is required for proliferation, but not differentiation.

PRC2 controls urothelial identity by preventing ectopic expression of squamous epithelial markers

Bladder urothelium differs significantly from other types of stratified epithelium with regards to the expression profile of cytokeratin family genes. Abnormal urothelial differentiation of *Eed* cKO^{Shh} mutants prompted us to examine whether PRC2 is required to establish the molecular identity of bladder urothelium. Normal murine urothelium expressed high levels of Krt5 in the basal cell layer at E18.5 (Fig. 4A and Fig. 5A). About 14% of Krt5^{+} urothelial cells also expressed *Krt14*, but *Krt17* expression was undetectable in normal urothelium (Fig. 5A,B). In *Eed* cKO^{Shh} mutants, both Krt14 (90%) and Krt17 (71%) were significantly elevated (Fig. 4A,B and Fig. 5A,B). These observations were confirmed independently by quantitative analysis of mRNA levels (Fig. 4C,D). In addition, *Krt1*, *Krt6a* and *Krt16* were significantly upregulated in the mutants (Fig. 4C,D). Previous studies have shown that vitamin A deficiency induces keratinizing squamous metaplasia of urothelium, including ectopic expression and expansion of Krt14^{+} basal cells (Liang et al., 2005; Molloy and Laskin, 1988). To examine whether the RA signaling pathway was affected in the

Development (2017) 144, 400-408 doi:10.1242/dev.143958

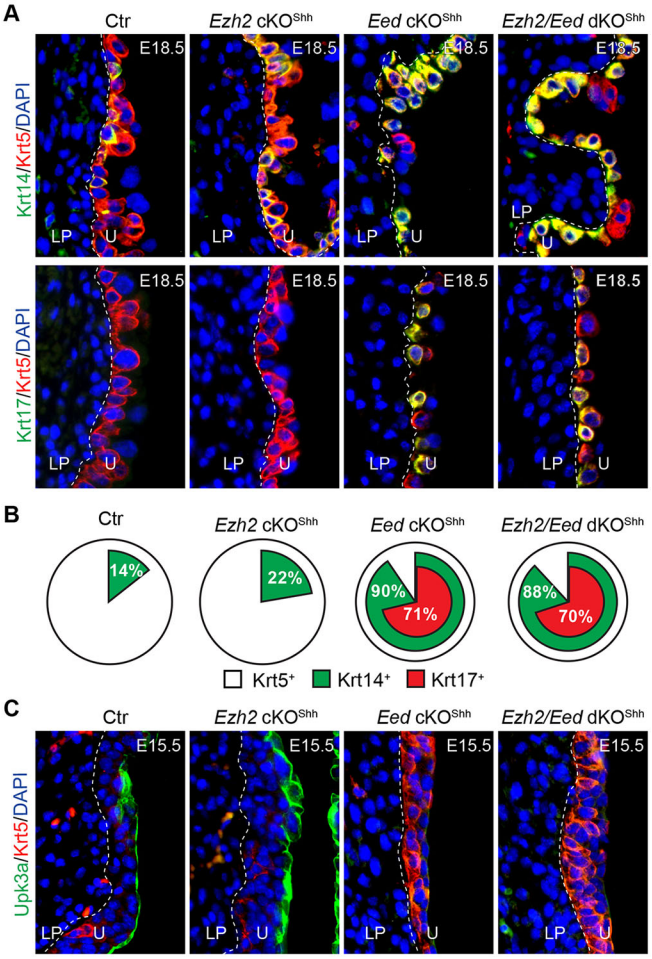

Fig. 5. *Eed* and *Ezh2* have distinct roles in urothelial differentiation. (A,B) Double immunofluorescence staining of bladder sections from control (Ctr, $Eed^{fl/+};Shh^{GC/+}$), *Ezh2* cKO^{Shh} ($Ezh2^{f/f};Shh^{GC/+}$), *Eed* cKO^{Shh} ($Eed^{f/f};Shh^{GC/+}$) and *Ezh2*/*Eed* double cKO^{Shh} (dKO^{Shh}, $Eed^{f/f};Ezh2^{f/f};Shh^{GC/+}$) embryos at E18.5 using antibodies against Krt5 (red) and Krt14 (green) or Krt5 (red) and Krt17 (green) (A). The results are summarized in B. (C) Double immunofluorescence staining of bladder sections from E15.5 embryos with indicated genotypes using antibodies against Krt5 (red) and Upk3a (green). LP, lamina propria; U, urothelium.

mutants, we examined expression of genes that are essential for RA metabolism. Expression of *Raldh2*, which catalyzes production of RA, was not affected. However, *Cyp26a1* and *Cyp26a2*, which encode enzymes that degrade RA, were significantly increased (Fig. 4E). Consistently, *Foxa1*, a downstream target of the RA signaling pathway (Jacob et al., 1994, 1999), was significantly decreased (Fig. 4F). Nuclear hormone receptor Pparg binds to DNA as a heterodimer with RA receptors (Kojetin et al., 2015), and *Pparg* gene expression inversely correlates with squamous differentiation of urothelium (Strand et al., 2013). *Pparg* was significantly downregulated in *Eed* cKO^{Shh} mutants (Fig. 4F). Collectively, these findings suggest that PRC2 controls urothelial identity by preventing squamous-like differentiation, possibly through modulation of the RA signaling pathway.

PRC2 subunit-specific functions in urothelial differentiation

Ezh2 is the major enzymatic subunit of the PRC2 complex and it is highly expressed in the urothelium (Fig. 1C). Consistently, H3K27me3 was undetectable from mutant urothelium in which *Ezh2* was conditionally deleted using the Shh^{GC} *Cre* driver (Fig. S7). Similar to the *Eed* mutants, *Ezh2* cKO^{Shh} mutants died after birth with defective lung development (Fig. S7A-D). The *Ezh2* cKO^{Shh} mutant urothelium was hypoplastic (Fig. S7F,G). *P16* expression was aberrantly upregulated and, consistent with this finding, cell proliferation rates were also significantly reduced (Fig. S7H-J). Interestingly, both *Eed* and *Ezh2* cKO^{Shh} mutants developed a polydactyly phenotype (Fig. S2G and Table S1). To examine whether *Ezh2* and *Eed* act synergistically *in vivo*, we generated compound cKO mice in which copies of *Eed* and *Ezh2* genes were deleted using Shh^{GC}. The gross polydactyly phenotype was observed in ∼11.3% of *Eed* heterozygous mutants but not in *Ezh2* heterozygous mutants. Penetrance of this phenotype was increased significantly to 36.4% in *Ezh2* and *Eed* double heterozygous mutants. Penetrance was further enhanced when additional alleles of *Ezh2* or *Eed* were deleted (Table S1). Collectively, these observations indicate that *Ezh2* and *Eed* are two integral components of the PRC2 complex with overlapping functions *in vivo*.

We also analyzed the urothelial differentiation phenotype in *Ezh2* cKO^{Shh} mutant bladders. While significantly more Krt14$^+$ cells were found within the Krt5$^+$ basal population in *Ezh2* cKO^{Shh} mutants (Fig. 5A,B) compared with wild-type controls at E18.5 (22% versus 14%, $P<0.01$), the percentage of Krt14$^+$ cells was more markedly increased to 90% and 88% in *Eed* and *Eed*/*Ezh2* double knockout mutants, respectively (Fig. 5A,B). Additionally, ectopic Krt17 expression was only observed in the *Eed* single and double knockouts but not in the *Ezh2* mutants (Fig. 5A,B). The dramatic difference in urothelial differentiation between *Ezh2* and *Eed* mutants prompted us to examine whether these PRC2 subunits also have different functions in regulating the timing of urothelial differentiation. We therefore analyzed the mutants at E15.5, which corresponds to the onset of urothelial differentiation. In contrast to *Eed* mutants, *Ezh2* conditional knockouts demonstrated a significant upregulation of Upk3a$^+$ superficial cells at E15.5 (Fig. 5C) whereas Krt5 expression was unaffected. We next examined whether *Ezh2* and *Eed* functionally depended on each other within the canonical PRC2 complex, or whether they act independently. Specifically, we compared expression of *Upk3a* and *Krt5* in wild-type controls, single knockout and double knockout animals at E15.5. As shown in Fig. 5C, *Upk3a* was upregulated in *Ezh2* mutants but was downregulated in both *Eed* mutants and double knockouts (*Ezh2*/*Eed* dKO^{Shh}). In addition, *Krt5* was dramatically upregulated in *Eed* and double knockout mutants but not in *Ezh2* mutants. Collectively, these findings suggest that, while the PRC2 subunits have overlapping functions in urothelial progenitor cell proliferation, the *Eed* and *Ezh2* subunits have unique roles in urothelial differentiation – *Eed* suppresses premature Krt5$^+$ basal cell differentiation but promotes Upk3a$^+$ superficial cell differentiation; *Ezh2*, however, has minimal effect on Krt5$^+$ basal cells while inhibiting premature Upk3a$^+$ superficial cell differentiation.

Eed is required to maintain the quiescent state of mature urothelium

We next examined the role of PRC2 in adult urothelial progenitors using Shh^{CreER} (Gandhi et al., 2013; Shen et al., 2008; Shin et al., 2011). The mutants $Shh^{CreER};Eed^{f/f};R26R^{lacZ}$, termed *Eed* icKO^{Shh}, were healthy and fertile. Tamoxifen treatment induced *Eed* gene deletion and activation the genetic lineage marker *lacZ* in a limited population of adult urothelial progenitors. This genetic mosaic approach was used to track and monitor individual *Eed* mutant urothelial progenitor prospectively thereby to assess regenerative

Development (2017) 144, 400-408 doi:10.1242/dev.143958

potential of urothelial progenitors. Specifically, the genetically tagged and *Eed* mutant progenitors (and their daughter cells) were analyzed by β-galactosidase (β-gal) staining 4-6 weeks after tamoxifen treatment (Fig. 6A, PBS). Most β-gal$^+$ cells in both control and *Eed* icKO^{Shh} mutants were small *Shh*$^+$ urothelial progenitor cells located at the basal or intermediate layers of urothelium (Fig. 6A,C). Very few large β-gal$^+$ superficial cells were observed in controls, confirming that adult urothelium is largely quiescent. However, the mutant urothelium demonstrated significantly more β-gal$^+$ superficial cells than controls (Fig. 6A, B), suggesting that *Eed* is required to maintain the quiescent state of mature urothelium by preventing precocious differentiation.

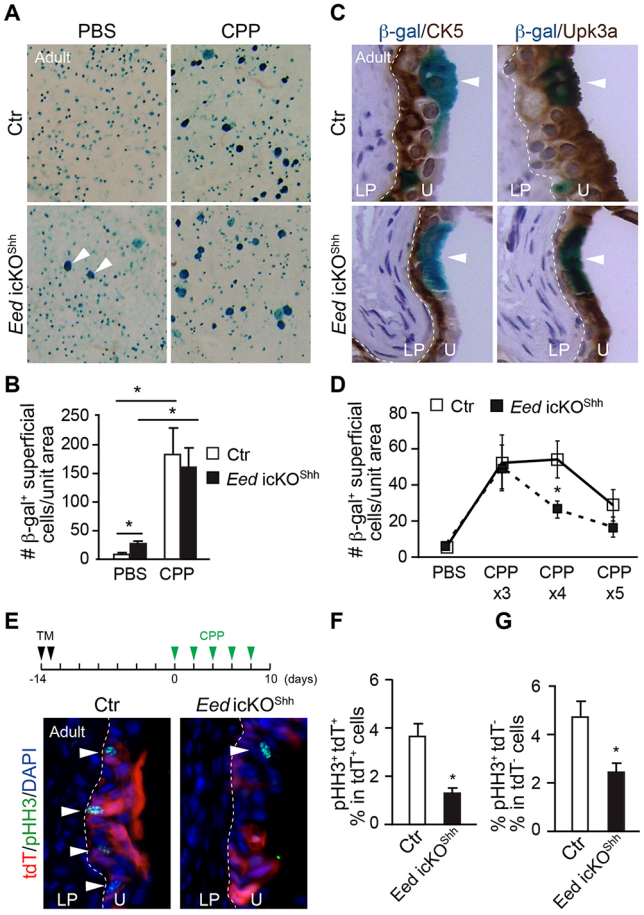

Fig. 6. *Eed* is required to maintain the quiescent state and regenerative capacity of *Shh*$^+$ adult urothelial progenitors. (A) Following tamoxifen treatment of *Shh*^{CreER}*Eed*$^{fl/+}$;*R26R*^{lacZ} control (Ctr) and *Shh*^{CreER};*Eed*$^{fl/fl}$;*R26R*^{lacZ} mutant (*Eed* icKO^{Shh}) mice to induce *Eed* deletion and/or reporter expression from *Shh*$^+$ urothelial progenitors, mice were treated with a single dose of PBS or CPP. Two weeks later, bladders were harvested, stained to detect β-gal, and whole mounts were made from urothelium. Following injury, small blue cells that include *Shh*$^+$ progenitor cells will differentiate to larger blue superficial cells (arrowheads). (B) Quantification of the number of β-gal$^+$ superficial cells per unit area in control or *Eed* icKO^{Shh} treated with a single dose of PBS or CPP (*n*=12-15 mice per group). (C) Immunohistochemical staining of adult control (Ctr) and *Eed* icKO^{Shh} bladders that have been tamoxifen induced, treated with a single dose of CPP, sectioned, and double stained for β-gal and Krt5 (brown; left panels) or Upk3a (brown; right panels). β-gal$^+$ superficial cells (white arrowheads) stain for Upk3a, and basal cells (red arrowheads) stain for Krt5. (D) Control and *Eed* icKO^{Shh} mice were tamoxifen induced and treated with 3-5 rounds of CPP. Two weeks after the last injury, the number of β-gal$^+$ superficial cells per unit area was calculated for each group (*n*=3-8 mice per group). (E) Control (*Shh*^{CE}*Eed*$^{fl/+}$;*R26R*^{tdT}) and *Eed* icKO^{Shh} mice expressing the *R26R*^{tdT} reporter (red) were tamoxifen (TM) induced and treated with five rounds of CPP. Forty-eight hours after the last injury, bladder sections were stained for pHH3 (green) to measure proliferation. Arrowheads indicate pHH3$^+$ cells. (F,G) The percentage of pHH3$^+$ cells that are tdT$^+$ within the total population of tdT$^+$ cells (F) and the percentage of pHH3$^+$ cells that are tdT$^-$ within the total population of tdT$^-$ cells (G). White dashed lines demarcate the different layers within the bladder (U, urothelium; LP, lamina propria). Data in B,D,F,G represent mean±s.e.m. Unpaired Student's *t*-test, **P*<0.05.

PRC2 regulates regenerative capacity of adult urothelial progenitors

To determine whether the PRC2-dependent epigenetic program is required for adult urothelial regeneration, we injured bladders with a single dose of the alkylating agent cyclophosphamide (CPP) 4 weeks after tamoxifen-induced deletion of *Eed* in *Shh*$^+$ urothelial progenitor cells (Gandhi et al., 2013; Shin et al., 2011). CPP is known to cause an acute urothelial injury with damaged urothelium regenerating rapidly and recovering completely within 7-10 days (Kunze et al., 1980). There was a significant increase in number of β-gal$^+$ large superficial cells 2 weeks post-CPP injury in control urothelium, confirming the complete cycle of urothelium injury and regeneration (Fig. 6A, top right panel, and B). Similar numbers of β-gal$^+$ superficial cells were observed in *Eed* icKO^{Shh} mutants after a single dose of CPP (Fig. 6A, bottom right panel, and B). However, after repeated CPP injury, significantly fewer β-gal$^+$ superficial cells were detected in mutant urothelium (Fig. 6D). Furthermore, cell proliferation was also reduced in the mutants during the regenerative process after repeated injury. Notably, this proliferation defect was not limited to the mutant cells (Fig. 6E-G), consistent with the notion that PRC2 has both cell-autonomous and non-autonomous functions in regulating urothelial proliferation. Collectively, these results suggest that PRC2 regulates the regenerative capacity of adult urothelium including progenitor cell proliferation and superficial cell differentiation.

DISCUSSION

In this study, we report for the first time that the PRC2-dependent epigenetic program regulates urothelial progenitor cell proliferation and timing of differentiation, and PRC2 controls the fate and regenerative potential of adult urothelial progenitors. These findings establish the crucial roles of the epigenetic program in urothelial development and adult urothelial homeostasis.

Bladder urothelium, one of the most effective epithelial barriers, is central to protecting the urinary tissue from toxic substances and pathogens in the urine. The urothelial cells change size and shape consistently during urine storage and voiding. Under physiological conditions, the urothelial cells have low turnover rate but regenerate rapidly upon injury. The bladder urothelium is thought to have three major cell types. Our observation that the PRC2-mediated H3K27me3 epigenetic mark is highly enriched and variable in the urothelium suggest the possibility that different levels of H3K27me3 may reflect diverse basal, intermediate and superficial cell types. Papafotiou et al. (2016) show that *Krt14* expression marks a subpopulation of murine bladder basal cells with essential roles in regeneration and tumorigenesis. Expression of *KRT14* is also linked to human bladder cancer development (Cancer Genome Atlas Research Network, 2014; Sjodahl et al., 2012; Volkmer et al., 2012). Interestingly, the Krt14$^+$ as well as the ectopic Krt17$^+$ sub-populations of basal cells are significantly increased in *Eed* mutants. In addition, *Eed* mutation causes downregulation of genes important for RA signaling pathways (e.g. *Cyp26a1*, *Cyp26b1*, *Foxa1* and *Pparg*). Consistent with our observations, inactivation of the RA

Development (2017) 144, 400-408 doi:10.1242/dev.143958

signaling pathway, through Vitamin A deficiency (Liang et al., 2005; Molloy and Laskin, 1988), Pparg knockdown (Strand et al., 2013) and *Foxa1* downregulation (Jacob et al., 1994, 1999) results in the squamous-like phenotype of bladder urothelium. Collectively, these findings strongly suggest that there is a significant cellular diversity of bladder urothelium with unique properties and functions for each cell type. Moreover, the PRC2-dependent epigenetic program plays an important role in the formation and maintenance of diverse urothelial cells.

The observation that PRC2 regulates the timing of urothelial progenitor cell differentiation is particularly intriguing. Deletion of *Eed* triggers premature differentiation of Krt5^{+} basal cells and a delay in Upk3a^{+} superficial cell formation. By contrast, *Ezh2* deletion increased *Upk3a* gene expression but had no apparent effect on *Krt5*. The phenotypic difference between *Eed* and *Ezh2* cKO mice is somewhat surprising given the global loss of H3K27me3 marks in the urothelium in both mutant lines. However, we could not rule out the possibility that H3K27me3 marks at discrete gene loci are actually preserved in *Ezh2* cKO^{shh} urothelial cells because of the compensatory effect of *Ezh1*, as shown in other organ systems including embryonic stem cells, hematopoietic cells and skin (Ezhkova et al., 2011; Shen et al., 2008; Xie et al., 2014). Indeed, our observation that *Eed*/*Ezh2* double cKO mice have an identical phenotype to *Eed* single cKO mice argues against the notion that *Ezh2* functions independent of *Eed* to prevent superficial cell differentiation. On the contrary, it is possible that *Eed* may have an independent function because, in addition to PRC2, *Eed* may also control PRC1 activity (Cao et al., 2014). Unlike other stratified epithelia, *Krt5* expression follows, rather than precedes, superficial and intermediate cell differentiation during normal bladder urothelium formation (Gandhi et al., 2013). The timing defect of urothelial differentiation seen in *Eed* and *Ezh2* cKO^{Shh} mutants indicates that, regardless of the lineage relationship, timing of basal and superficial cell differentiation may vary depending on the genetic background and epigenetic landscape.

Consistent with the essential roles of PRC2 in progenitor cell proliferation through repression of cell cycle inhibitors such as *Cdkn2a*, we have observed a significant increase in *Cdkn2a* gene expression with a reduction in urothelial cell proliferation of *Eed* cKO^{Shh} embryos. Moreover, we provide evidence that PRC2 indirectly promotes *Shh* expression in the urothelium by repressing *Pax6*, a known transcriptional repressor of *Shh* (Caballero et al., 2014). Feedback regulation between *Shh* and *Wnt* signals is essential for the regenerative proliferation of urothelial progenitors (Shin et al., 2011). In addition, *in vitro* and *in vivo* studies have underscored the importance of urothelial *Shh* in patterning of the bladder wall and in the proliferation and differentiation of SMCs (Cao et al., 2010; Haraguchi et al., 2007). This is consistent with our finding that *Eed* cKO bladders exhibit decreased LP and SMC proliferation as well as aberrant SMC differentiation. Therefore, PRC2 exerts both cell-autonomous and non-autonomous functions in bladder urothelium by regulating the expression of genes including cell cycle regulators, transcription factors and signaling molecules.

Using a chemical-induced bladder injury model, we found that PRC2 regulates the regenerative capacity of Shh^{+} adult urothelial progenitors. Adult Shh^{+} urothelial progenitors deleted in *Eed* precociously differentiate into superficial cells, indicating that PRC2 is required to maintain the quiescent state of adult urothelium under normal physiological conditions. Upon chemical-induced injury, we show that the proliferation rate of Shh^{+} urothelial progenitors is significantly reduced in the absence of *Eed*. Moreover, the ability of mutant progenitors to generate superficial cells is significantly reduced after repeated injuries. Urothelial regeneration is essential for barrier function to protect the urinary tract, and aberrant regenerative responses may predispose to neoplastic transformation and, in the case of urinary tract infection, to chronic and ascending infections (Mysorekar et al., 2009; Shin et al., 2011). Our findings highlight the essential roles of epigenetic regulation of urothelial formation and regeneration (Fig. 7), which may provide a new framework for understanding the molecular basis of urinary tract infection and tumorigenesis.

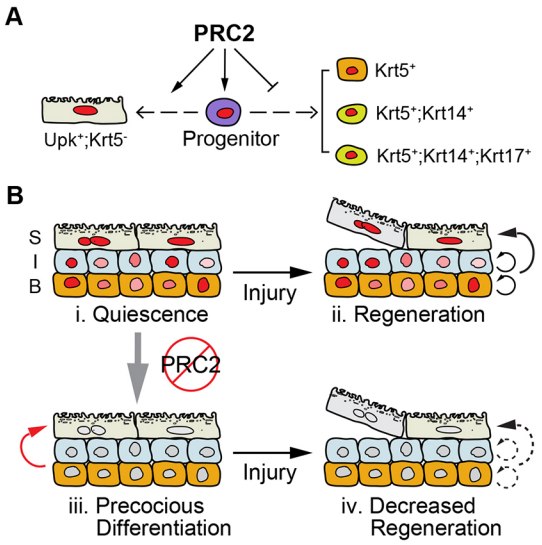

Fig. 7. PRC2 regulates bladder urothelium development, maintenance and regeneration. (A) PRC2 promotes proliferation of embryonic urothelial progenitor cells. Moreover, PRC2 controls urothelial differentiation by inhibiting premature differentiation of Krt5^{+} basal cells and preventing ectopic expression of Krt14 and Krt17. Conversely, PRC2 may promote differentiation of Upk3a^{+} superficial cells. (B) PRC2 is required to maintain the quiescent state (i) and regenerative potential (ii) of adult urothelial progenitors. Without PRC2, adult urothelial progenitors (e.g. the Shh^{+} urothelial progenitors) precociously differentiate to superficial cells (iii, red arrow). However, their ability to repeatedly form superficial cells is limited (iv, dashed arrows).

MATERIALS AND METHODS

Mouse strains

The bladder urothelium-specific *Ezh2* or *Eed* conditional knockout embryos/mice were generated by crossing either *Shh*^{GC} (Harfe et al., 2004) (Jackson Laboratory, 005622) or *Upk2-Cre* Cre drivers (Kanasaki et al., 2013) with *Ezh2*$^{f/f}$ or *Eed*$^{f/f}$ conditional alleles (Shen et al., 2008; Xie et al., 2014) (obtained from Dr Stuart Orkin, Boston Children's Hospital, Harvard Medical School). Double cKO mice and littermate controls were generated by crossing *Shh*^{GC};*Ezh2*$^{f/+}$;*Eed*$^{f/+}$ mice with *Ezh2*$^{f/f}$;*Eed*$^{f/f}$ mice. *Upk2-Cre* mice were crossed with *Rosa26Sor*$^{CAG\text{-}tdTomatoRed}$ mice (Jackson Laboratory, 007905) to generate *Upk2-Cre;R26R*^{tdT} reporter mice for lineage tracing experiments. *Eed* tamoxifen-inducible cKO mice (*Shh*^{CreER};*Eed*$^{f/f}$) were crossed with mice carrying either the *R26R*^{lacZ} (003309) or *R26R*^{tdT} genes to generate *Shh*^{CreER};*Eed*$^{f/f}$;*R26R*^{lacZ} or *Shh*^{CreER};*Eed*$^{f/f}$;*R26R*^{tdT} reporter mice, respectively. Controls used throughout the study were compound heterozygous with one allele of the Cre driver and one conditional allele. There was no detectable gender difference in phenotype, therefore, male and female mice were used interchangeably in the study. All animal studies were performed according to protocols reviewed and approved by the Institutional Animal Care and Use Committee at Boston Children's Hospital.

Development (2017) 144, 400-408 doi:10.1242/dev.143958

Histology, immunohistochemistry and TUNEL staining

For histological examination, tissues were fixed in 4% paraformaldehyde (PFA), embedded in either paraffin or OCT medium, and sectioned at a thickness of 4-10 µm. Hematoxylin and Eosin (H&E, Thermo Fisher Scientific) staining was performed on paraffin sections according to standard protocol. Paraffin sections and/or cryostat sections were used for immunohistochemistry. After blocking sections in 10% goat serum/10% BSA for 1 h at room temperature, sections were incubated overnight at 4°C with the following primary antibodies: anti-Krt5 (Abcam, ab53121, 1:500 and Covance, SIG-3475, 1:1000), anti-Krt14 (Santa Cruz, SC-53253, 1:100), anti-Krt17 (Santa Cruz, SC-101931, 1:100), anti-Upk3a (Hu et al., 2005; Liang et al., 2001) (Clone AU1, provided by Dr Tung-Tien Sun, New York University, 1:200), anti-H3K27me3 (Millipore, 07-449, 1:200), anti-SMA (Sigma, A2547, 1:200), and anti-pHH3 (Upstate, 06-570, 1:200). Fluorescently labeled donkey anti-mouse or anti-rabbit secondary antibodies (Jackson ImmunoResearch, 1:200) were incubated for 1 h at room temperature. All sections were counterstained with DAPI. For immunohistochemical staining with DAB, an HRP-conjugated goat anti-rabbit or anti-mouse secondary antibody (Abcam, 1:500) was used followed by development with the DAB peroxidase substrate kit (Vector Laboratories) according to the manufacturer's instructions. To measure apoptosis, TUNEL staining was performed on paraffin sections using the *In Situ* Cell Death Detection Kit (Roche) according to manufacturer's instructions. Imaging was performed using a Zeiss fluorescence microscope.

Genetic mosaic analysis

Shh^{CreER};$Eed^{f/f}$;$R26R^{lacZ}$ or Shh^{CreER};$Eed^{f/f}$;$R26R^{tdT}$ mutants and compound heterozygous controls (Shh^{CreER};$Eed^{f/+}$;$R26R^{lacZ}$ or Shh^{CreER};$Eed^{f/+}$;$R26R^{tdT}$) mice were intraperitoneally injected with tamoxifen (150 µg/g body weight; Sigma T5648) once daily for 2 days between ages P30-P60. Two weeks later, mice were intraperitoneally injected with either PBS or CPP (150 µg/g body weight, Sigma C7397). Analyses were performed at either 48 h for proliferation studies or at 2 weeks after CPP injection for regeneration studies, as indicated in the text. Specifically, β-gal staining was performed after bisecting bladder along the midline sagittal plane. Whole mounts of microdissected urothelium from bladder halves were then prepared and imaged. Using ImageJ software, β-gal$^+$ superficial cells were counted based on their large size, polyhedral shape, and/or Upk3a$^+$ staining. Each sample was normalized against total surface area of urothelium.

RNA isolation and qRT-PCR

Total RNA was extracted from either whole bladders or microdissected urothelium using the RNeasy Plus Mini Kit (Qiagen). Genomic DNA was removed using gDNA Eliminator spin columns (Qiagen). Total RNA was reverse-transcribed into cDNA using the SuperScript III Reverse Transcriptase Kit (Invitrogen). Quantitative real-time PCR (qRT-PCR) analyses were performed using SYBR Green (Roche) on an ABI-7500 detector (Applied Biosystems). Relative gene expression levels were normalized to the internal control *Gapdh*. Gene-specific primers are shown in Table S2.

In situ hybridization

Whole-mount *in situ* hybridization of control and mutant embryos was performed as previously described (Guo et al., 2014, 2011; Li et al., 2002), using digoxigenin-labeled RNA probes against *Shh* and *Pax6*.

Chromatin immunoprecipitation assays

Chromatin immunoprecipitation was performed as previously described (Guo et al., 2011). Briefly, microdissected urothelial cells from ∼15-20 bladders per group were crosslinked with 1% formaldehyde at room temperature for 15 min. Cells were then lysed and sonicated to an average size of 500-1000 base pairs. Chromatin lysates were incubated with specific antibodies (1 µg per reaction) including Ezh2 (Cell Signaling, 5246), H3K4me3 (Motif Active, 39159), or control IgG. Immunoprecipitates were collected with Protein G Dynabeads (Invitrogen) and protein/DNA crosslinks were reversed with 5 M NaCl. DNA was purified and ChIP DNA was analyzed using qPCR as described above. Each sample was normalized against total DNA input. The gene-specific primers used are listed in Table S3.

Statistical analyses

For all graphs, data are presented as the mean±s.e.m. Either the unpaired two-tailed Student's *t*-test or the unpaired Mann–Whitney test was used to determine significance between two groups, as indicated in the Results. *P*-values <0.05 were considered statistically significant.

Acknowledgements

We thank Roslyn Adam, Joshua Mauney and Satoshi Kaneko for helpful discussions and comments.

Competing interests

The authors declare no competing or financial interests.

Author contributions

Conceptualization: X.L.; Methodology: X.L., C.G., Z.R.B.; Formal analysis and investigation: C.G., Z.R.B.; Writing - original draft preparation: Z.R.B., C.G.; Writing - review and editing: X.L., Z.R.B., C.G.; Funding acquisition: X.L., C.G., Z.R.B.; Resources: X.L., W.G.H.; Supervision: X.L.

Funding

This work was supported by American Urological Association scholar awards (to C.G. and Z.R.B.), National Institute of Diabetes and Digestive and Kidney Diseases (1R01DK091645-01A1 to X.L.), National Cancer Institute (1R21CA198544 to X.L.) and the American Heart Association (13GRNT16950006). Deposited in PMC for release after 12 months.

Supplementary information

Supplementary information available online at
http://dev.biologists.org/lookup/doi/10.1242/dev.143958.supplemental

References

Caballero, I. M., Manuel, M. N., Molinek, M., Quintana-Urzainqui, I., Mi, D., Shimogori, T. and Price, D. J. (2014). Cell-autonomous repression of Shh by transcription factor Pax6 regulates diencephalic patterning by controlling the central diencephalic organizer. *Cell Rep.* **8**, 1405-1418.

Cancer Genome Atlas Research Network (2014). Comprehensive molecular characterization of urothelial bladder carcinoma. *Nature* **507**, 315-322.

Cao, R., Wang, L., Wang, H., Xia, L., Erdjument-Bromage, H., Tempst, P., Jones, R. S. and Zhang, Y. (2002). Role of histone H3 lysine 27 methylation in Polycomb-group silencing. *Science* **298**, 1039-1043.

Cao, M., Tasian, G., Wang, M.-H., Liu, B., Cunha, G. and Baskin, L. (2010). Urothelium-derived Sonic hedgehog promotes mesenchymal proliferation and induces bladder smooth muscle differentiation. *Differentiation* **79**, 244-250.

Cao, Q., Wang, X., Zhao, M., Yang, R., Malik, R., Qiao, Y., Poliakov, A., Yocum, A. K., Li, Y., Chen, W. et al. (2014). The central role of EED in the orchestration of polycomb group complexes. *Nat. Commun.* **5**, 3127.

Colopy, S. A., Bjorling, D. E., Mulligan, W. A. and Bushman, W. (2014). A population of progenitor cells in the basal and intermediate layers of the murine bladder urothelium contributes to urothelial development and regeneration. *Dev. Dyn.* **243**, 988-998.

Czermin, B., Melfi, R., McCabe, D., Seitz, V., Imhof, A. and Pirrotta, V. (2002). Drosophila enhancer of Zeste/ESC complexes have a histone H3 methyltransferase activity that marks chromosomal Polycomb sites. *Cell* **111**, 185-196.

Delgado-Olguín, P., Huang, Y., Li, X., Christodoulou, D., Seidman, C. E., Seidman, J. G., Tarakhovsky, A. and Bruneau, B. G. (2012). Epigenetic repression of cardiac progenitor gene expression by Ezh2 is required for postnatal cardiac homeostasis. *Nat. Genet.* **44**, 343-347.

DeSouza, K. R., Saha, M., Carpenter, A. R., Scott, M. and McHugh, K. M. (2013). Analysis of the Sonic Hedgehog signaling pathway in normal and abnormal bladder development. *PLoS ONE* **8**, e53675.

Ezhkova, E., Lien, W.-H., Stokes, N., Pasolli, H. A., Silva, J. M. and Fuchs, E. (2011). EZH1 and EZH2 cogovern histone H3K27 trimethylation and are essential for hair follicle homeostasis and wound repair. *Genes Dev.* **25**, 485-498.

Galvis, L. A., Holik, A. Z., Short, K. M., Pasquet, J., Lun, A. T. L., Blewitt, M. E., Smyth, I. M., Ritchie, M. E. and Asselin-Labat, M.-L. (2015). Repression of Igf1 expression by Ezh2 prevents basal cell differentiation in the developing lung. *Development* **142**, 1458-1469.

Gandhi, D., Molotkov, A., Batourina, E., Schneider, K., Dan, H., Reiley, M., Laufer, E., Metzger, D., Liang, F., Liao, Y. et al. (2013). Retinoid signaling in

progenitors controls specification and regeneration of the urothelium. *Dev. Cell* **26**, 469-482.
Georgas, K. M., Armstrong, J., Keast, J. R., Larkins, C. E., McHugh, K. M., Southard-Smith, E. M., Cohn, M. J., Batourina, E., Dan, H., Schneider, K. et al. (2015). An illustrated anatomical ontology of the developing mouse lower urogenital tract. *Development* **142**, 1893-1908.
Guo, C., Sun, Y., Zhou, B., Adam, R. M., Li, X. K., Pu, W. T., Morrow, B. E., Moon, A. and Li, X. (2011). A Tbx1-Six1/Eya1-Fgf8 genetic pathway controls mammalian cardiovascular and craniofacial morphogenesis. *J. Clin. Invest.* **121**, 1585-1595.
Guo, C., Sun, Y., Guo, C., MacDonald, B. T., Borer, J. G. and Li, X. (2014). Dkk1 in the peri-cloaca mesenchyme regulates formation of anorectal and genitourinary tracts. *Dev. Biol.* **385**, 41-51.
Haraguchi, R., Motoyama, J., Sasaki, H., Satoh, Y., Miyagawa, S., Nakagata, N., Moon, A. and Yamada, G. (2007). Molecular analysis of coordinated bladder and urogenital organ formation by Hedgehog signaling. *Development* **134**, 525-533.
Harfe, B. D., Scherz, P. J., Nissim, S., Tian, H., McMahon, A. P. and Tabin, C. J. (2004). Evidence for an expansion-based temporal Shh gradient in specifying vertebrate digit identities. *Cell* **118**, 517-528.
He, A., Ma, Q., Cao, J., von Gise, A., Zhou, P., Xie, H., Zhang, B., Hsing, M., Christodoulou, D. C., Cahan, P. et al. (2012). Polycomb repressive complex 2 regulates normal development of the mouse heart. *Circ. Res.* **110**, 406-415.
Hu, C.-C. A., Liang, F.-X., Zhou, G., Tu, L., Tang, C.-H. A., Zhou, J., Kreibich, G. and Sun, T.-T. (2005). Assembly of urothelial plaques: tetraspanin function in membrane protein trafficking. *Mol. Biol. Cell* **16**, 3937-3950.
Huang, Y. C., Chen, F. and Li, X. (2016). Clarification of mammalian cloacal morphogenesis using high-resolution episcopic microscopy. *Dev. Biol.* **409**, 106-113.
Indra, A. K., Warot, X., Brocard, J., Bornert, J.-M., Xiao, J.-H., Chambon, P. and Metzger, D. (1999). Temporally-controlled site-specific mutagenesis in the basal layer of the epidermis: comparison of the recombinase activity of the tamoxifen-inducible Cre-ER(T) and Cre-ER(T2) recombinases. *Nucleic Acids Res.* **27**, 4324-4327.
Jacob, A., Budhiraja, S., Qian, X., Clevidence, D., Costa, R. H. and Reichel, R. R. (1994). Retinoic acid-mediated activation of HNF-3 alpha during EC stem cell differentiation. *Nucleic Acids Res.* **22**, 2126-2133.
Jacob, A., Budhiraja, S. and Reichel, R. R. (1999). The HNF-3alpha transcription factor is a primary target for retinoic acid action. *Exp. Cell Res.* **250**, 1-9.
Jost, S. P. (1989). Cell cycle of normal bladder urothelium in developing and adult mice. *Virchows Arch. B Cell Pathol. Incl. Mol. Pathol.* **57**, 27-36.
Kanasaki, K., Yu, W., von Bodungen, M., Larigakis, J. D., Kanasaki, M., Ayala de la Pena, F., Kalluri, R. and Hill, W. G. (2013). Loss of beta1-integrin from urothelium results in overactive bladder and incontinence in mice: a mechanosensory rather than structural phenotype. *FASEB J.* **27**, 1950-1961.
Kojetin, D. J., Matta-Camacho, E., Hughes, T. S., Srinivasan, S., Nwachukwu, J. C., Cavett, V., Nowak, J., Chalmers, M. J., Marciano, D. P., Kamenecka, T. M. et al. (2015). Structural mechanism for signal transduction in RXR nuclear receptor heterodimers. *Nat. Commun.* **6**, 8013.
Kunze, E., Engelhardt, W., Steinröder, H., Wöltjen, H.-H. and Schauer, A. (1980). Proliferation kinetics of regenerating urothelial cells in the rat urinary bladder after administration of cyclophosphamide (author's transl). *Virchows Archiv. B Cell Pathol. Incl. Mol. Pathol.* **33**, 47-66.
Kuzmichev, A., Nishioka, K., Erdjument-Bromage, H., Tempst, P. and Reinberg, D. (2002). Histone methyltransferase activity associated with a human multiprotein complex containing the Enhancer of Zeste protein. *Genes Dev.* **16**, 2893-2905.
Li, X., Perissi, V., Liu, F., Rose, D. W. and Rosenfeld, M. G. (2002). Tissue-specific regulation of retinal and pituitary precursor cell proliferation. *Science* **297**, 1180-1183.
Liang, F.-X., Riedel, I., Deng, F.-M., Zhou, G., Xu, C., Wu, X.-R., Kong, X.-P., Moll, R. and Sun, T.-T. (2001). Organization of uroplakin subunits: transmembrane topology, pair formation and plaque composition. *Biochem. J.* **355**, 13-18.
Liang, F.-X., Bosland, M. C., Huang, H., Romih, R., Baptiste, S., Deng, F.-M., Wu, X.-R., Shapiro, E. and Sun, T.-T. (2005). Cellular basis of urothelial squamous metaplasia: roles of lineage heterogeneity and cell replacement. *J. Cell Biol.* **171**, 835-844.
Margueron, R. and Reinberg, D. (2011). The Polycomb complex PRC2 and its mark in life. *Nature* **469**, 343-349.
Mauney, J. R., Ramachandran, A., Yu, R. N., Daley, G. Q., Adam, R. M. and Estrada, C. R. (2010). All-trans retinoic acid directs urothelial specification of murine embryonic stem cells via GATA4/6 signaling mechanisms. *PLoS ONE* **5**, e11513.
Molloy, C. J. and Laskin, J. D. (1988). Effect of retinoid deficiency on keratin expression in mouse bladder. *Exp. Mol. Pathol.* **49**, 128-140.
Montgomery, N. D., Yee, D., Chen, A., Kalantry, S., Chamberlain, S. J., Otte, A. P. and Magnuson, T. (2005). The murine polycomb group protein Eed is required for global histone H3 lysine-27 methylation. *Curr. Biol.* **15**, 942-947.
Müller, J., Hart, C. M., Francis, N. J., Vargas, M. L., Sengupta, A., Wild, B., Miller, E. L., O'Connor, M. B., Kingston, R. E. and Simon, J. A. (2002). Histone methyltransferase activity of a Drosophila Polycomb group repressor complex. *Cell* **111**, 197-208.
Mysorekar, I. U., Isaacson-Schmid, M., Walker, J. N., Mills, J. C. and Hultgren, S. J. (2009). Bone morphogenetic protein 4 signaling regulates epithelial renewal in the urinary tract in response to uropathogenic infection. *Cell Host Microbe* **5**, 463-475.
Papafotiou, G., Paraskevopoulou, V., Vasilaki, E., Kanaki, Z., Paschalidis, N. and Klinakis, A. (2016). KRT14 marks a subpopulation of bladder basal cells with pivotal role in regeneration and tumorigenesis. *Nat. Commun.* **7**, 11914.
Seifert, A. W., Harfe, B. D. and Cohn, M. J. (2008). Cell lineage analysis demonstrates an endodermal origin of the distal urethra and perineum. *Dev. Biol.* **318**, 143-152.
Shen, X., Liu, Y., Hsu, Y.-J., Fujiwara, Y., Kim, J., Mao, X., Yuan, G.-C. and Orkin, S. H. (2008). EZH1 mediates methylation on histone H3 lysine 27 and complements EZH2 in maintaining stem cell identity and executing pluripotency. *Mol. Cell* **32**, 491-502.
Shin, K., Lee, J., Guo, N., Kim, J., Lim, A., Qu, L., Mysorekar, I. U. and Beachy, P. A. (2011). Hedgehog/Wnt feedback supports regenerative proliferation of epithelial stem cells in bladder. *Nature* **472**, 110-114.
Shiroyanagi, Y., Liu, B., Cao, M., Agras, K., Li, J., Hsieh, M. H., Willingham, E. J. and Baskin, L. S. (2007). Urothelial sonic hedgehog signaling plays an important role in bladder smooth muscle formation. *Differentiation* **75**, 968-977.
Sjodahl, G., Lauss, M., Lovgren, K., Chebil, G., Gudjonsson, S., Veerla, S., Patschan, O., Aine, M., Ferno, M., Ringner, M. et al. (2012). A molecular taxonomy for urothelial carcinoma. *Clin. Cancer Res.* **18**, 3377-3386.
Snitow, M. E., Li, S., Morley, M. P., Rathi, K., Lu, M. M., Kadzik, R. S., Stewart, K. M. and Morrisey, E. E. (2015). Ezh2 represses the basal cell lineage during lung endoderm development. *Development* **142**, 108-117.
Strand, D. W., DeGraff, D. J., Jiang, M., Sameni, M., Franco, O. E., Love, H. D., Hayward, W. J., Lin-Tsai, O., Wang, A. Y., Cates, J. M. M. et al. (2013). Deficiency in metabolic regulators PPARgamma and PTEN cooperates to drive keratinizing squamous metaplasia in novel models of human tissue regeneration. *Am. J. Pathol.* **182**, 449-459.
Volkmer, J.-P., Sahoo, D., Chin, R. K., Ho, P. L., Tang, C., Kurtova, A. V., Willingham, S. B., Pazhanisamy, S. K., Contreras-Trujillo, H., Storm, T. A. et al. (2012). Three differentiation states risk-stratify bladder cancer into distinct subtypes. *Proc. Natl. Acad. Sci. USA* **109**, 2078-2083.
Xie, H., Xu, J., Hsu, J. H., Nguyen, M., Fujiwara, Y., Peng, C. and Orkin, S. H. (2014). Polycomb repressive complex 2 regulates normal hematopoietic stem cell function in a developmental-stage-specific manner. *Cell Stem Cell* **14**, 68-80.

SUPPLEMENTARY FIGURES

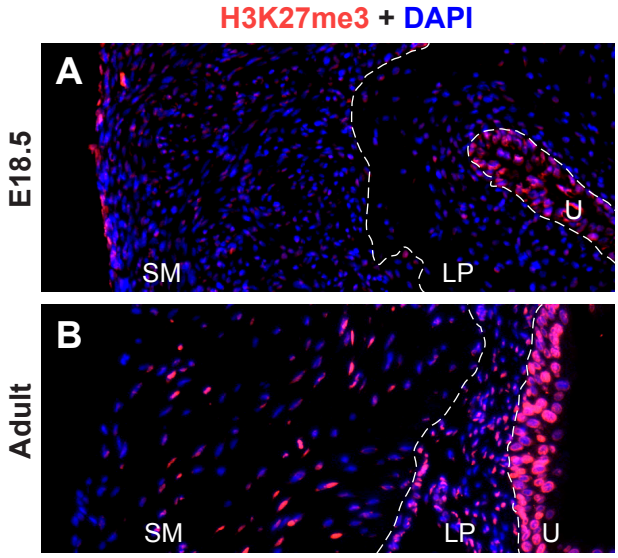

Figure S1. Epigenetic H3K27me3 modification is enriched in bladder urothelium. Immunofluorescence microscopy of bladder sections from wild type C57BL6 embryonic (E) day 18.5 (A) and adult (B) bladders stained with H3K27me3-specific antibody (red). Blue, DAPI counter staining. SM, smooth muscle layer; LP, lamina propria layer; and U, urothelial layer; white dash lines, boundaries of bladder tissue layers.

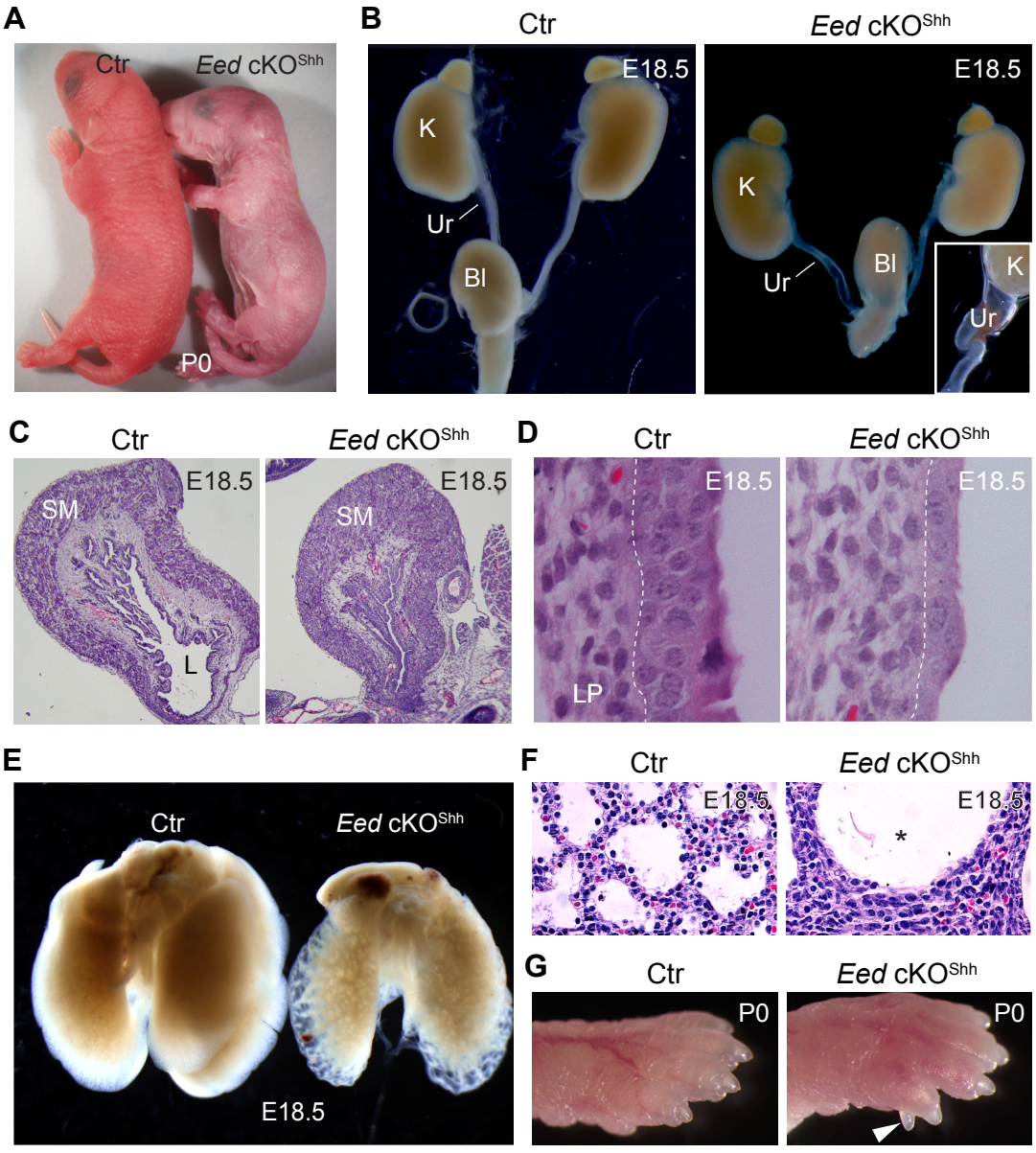

Figure S2. *Eed* cKO^{Shh} mice display early post-natal lethality with lung, limb, and genitourinary anomalies. (A) *Eed* cKO^{Shh} mutants die shortly after birth. (B) The genitourinary tract dissected from control (Ctr) and *Eed* cKO^{Shh} embryos at E18.5. Varying degrees of hydroureter (Ur, ureter) and/or hydronephrosis were appreciated in *Eed* cKO^{Shh} mutants (inset). Bl, bladder; K, kidney. (C-D) H&E staining of control and *Eed* cKO^{Shh} bladders at E18.5 reveals a reduction in overall thickness of the urothelium in the absence of *Eed*. (E) Lungs are visibly smaller in *Eed* cKO^{Shh} mice with enhanced lucency. (F) H&E staining of control and *Eed* cKO^{Shh} lungs at E18.5 reveals abnormal lung development with increased amounts of mesenchymal tissue between abnormally distended air sacs (asterisk). (G) The majority of *Eed* cKO^{Shh} embryos displayed unilateral or bilateral rudimentary postaxial accessory digits (arrowhead).

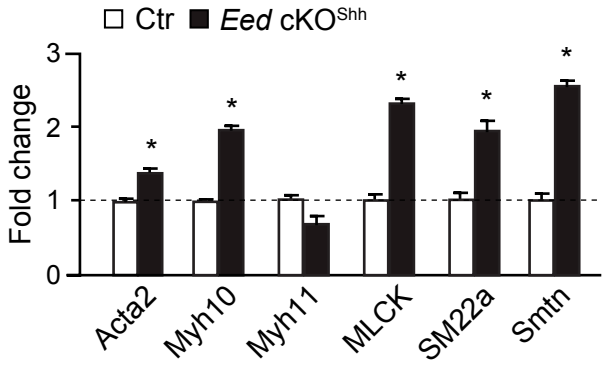

Figure S3. Loss of *Eed* in bladder urothelium leads to aberrant smooth muscle cell differentiation. qRT-PCR analysis of smooth muscle gene expression relative to *GAPDH* in whole bladders from E18.5 *Eed* cKO^{Shh} embryos normalized to controls. Data represent mean +/- s.e.m. Unpaired Student's *t*-test, **p* <0.05.

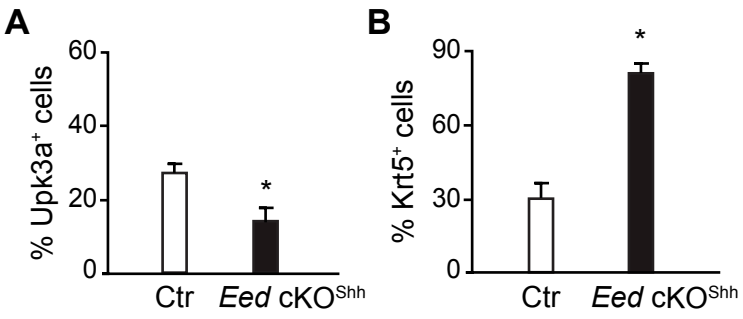

Figure S4. *Eed* cKO^{Shh} mutant urothelium has a significant reduction in Upk3a^{+} superficial cells and an increase in Krt5^{+} basal cells. Quantification analyses of immunofluorescence data shown in Figure 3A show the percentage of Upk3a^{+} cells (A) and Krt5^{+} cells (B) relative to total urothelial cells in E15.5 control versus *Eed* cKO^{Shh} embryos. Data represent mean +/- s.e.m. Unpaired Student's *t*-test, **p* <0.05.

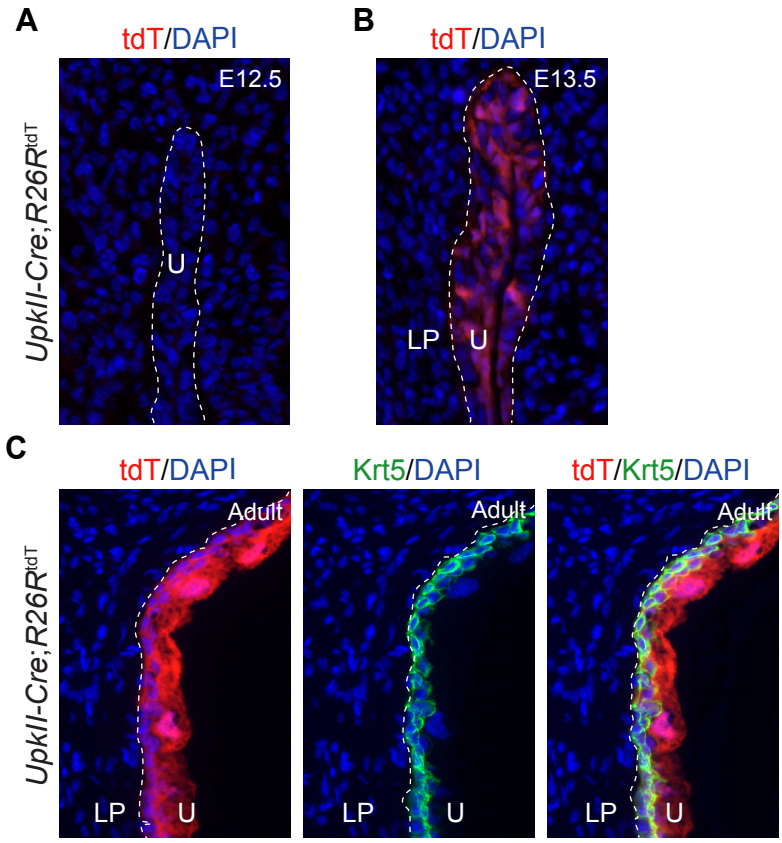

Figure S5. Cre activity of *Upk2-Cre* transgenic mice is detected in all layers of urothelium starting at E13.5. Lineage tracing experiments in bladder urothelium from E12.5 (A), E13.5 (B), and adult (C) *Upk2-Cre;R26R*^{tdT} reporter mice. Cells expressing the tomato red lineage marker (tdT) are shown in red. Bladder sections were also co-stained for Krt5 (green) and DAPI (blue). White dashed lines demarcate the different layers within the bladder (U, urothelium; LP, lamina propria).

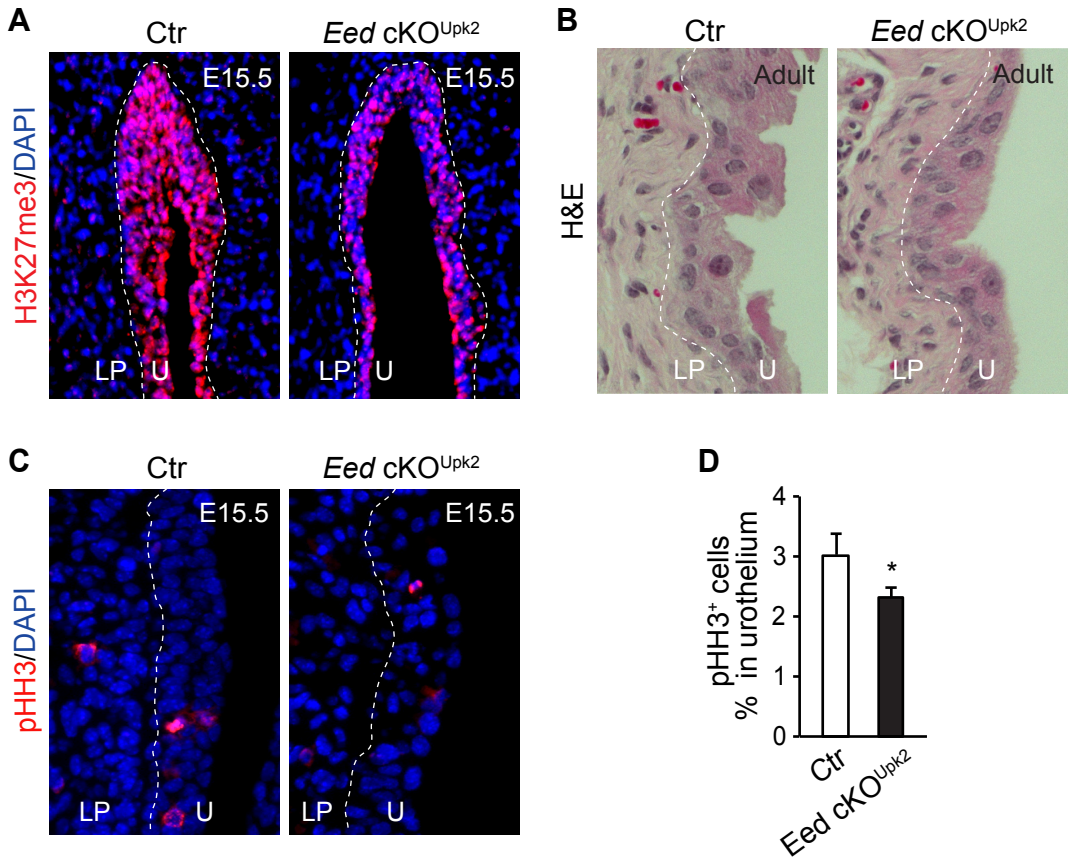

Figure S6. Deletion of *Eed* using *Upk2-Cre* reduces overall H3K27me3 level and urothelial proliferation rate at E15.5. (A) Bladder sections from control and *Eed* cKO^{Upk2} mice at E15.5 stained for H3K27me3 (red) and DAPI (blue). (B) H&E staining of adult control and *Eed* cKO^{Upk2} bladders. (C and D) Bladders from E15.5 control and *Eed* cKO^{Upk2} embryos stained for pHH3 (red) and DAPI (blue) and quantification of the data is shown in D. White dashed lines demarcate the different layers within the bladder (U, urothelium; LP, lamina propria). Data in D represent mean +/- s.e.m. Unpaired Student's *t*-test, **p* <0.05.

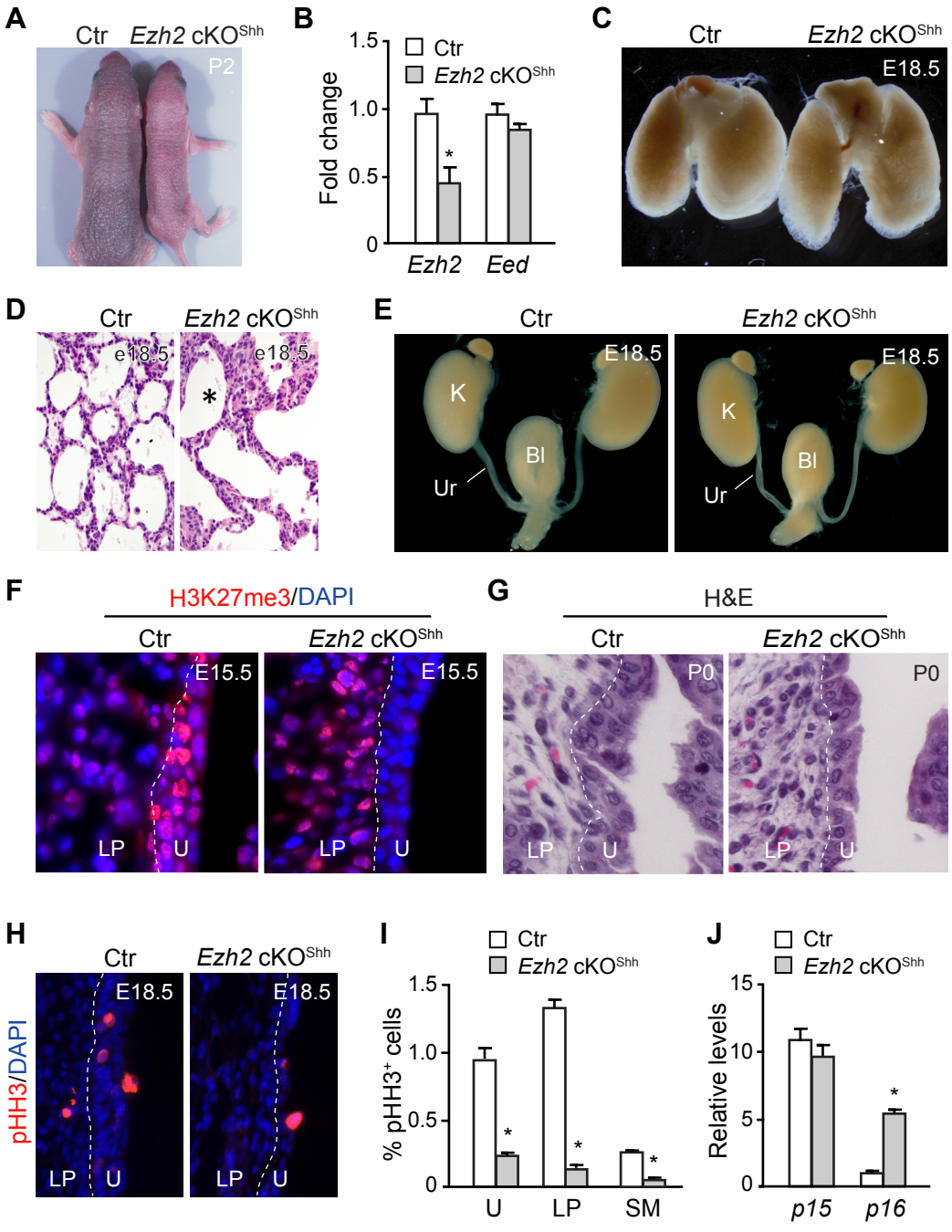

Figure S7. Conditional deletion of *Ezh2* in urothelium leads to a similar but milder phenotype compared conditional deletion of *Eed*. (A) *Ezh2* cKO^{Shh} mice are smaller than littermate controls at post-natal day 2 (P2) and die within 7 days of birth. (B) qRT-PCR analysis of microdissected urothelium at E18.5 from *Ezh2* cKO^{Shh} embryos normalized to control (Ctr). (C) Lungs of *Ezh2* cKO^{Shh} mice are similar in size to controls but display mild peripheral lucency as seen in *Eed* cKO^{Shh} lungs. (D) H&E staining of control and *Ezh2* cKO^{Shh} lungs at E18.5 confirm increased amounts of mesenchymal tissue between abnormally distended air sacs (asterisk). (E) The genitourinary tract dissected from control versus *Ezh2* cKO^{Shh} embryos at E18.5 reveals no gross differences in the

kidneys (K), ureters (Ur), and bladders (Bl) between both sets of animals. (F) Immunofluorescence microscopy of bladder sections from E15 control versus *Ezh2* cKO^{Shh} embryos stained with H3K27me3 (red) and DAPI (blue). (G) H&E staining of bladder sections from P0 control versus *Ezh2* cKO^{Shh} mice. (H) Immunofluorescence microscopy of bladder sections from control and *Ezh2* cKO^{Shh} animals at E18.5 stained for pHH3 (red) and DAPI (blue) with quantification of pHH3^{+} cells in I. (J) qRT-PCR analysis of *p15* and *p16* expression relative to *GAPDH* in microdissected urothelium from E18.5 control versus *Ezh2* cKO^{Shh} embryos White dashed lines demarcate the different layers within the bladder (U, urothelium; LP, lamina propria). Data in B, I, and J represent mean +/- s.e.m. Unpaired Student's *t*-test, **p* <0.05.

Supplemental Table 1: Limb phenotype (rudimentary postaxial accessory digit) in *Shh*^{GC}-mediated conditional *Eed* and *Ezh2* single and compound mutants

Genotype	total	limb defect	limb defect (%)
Eed$^{+/+}$;*Ezh2*$^{+/+}$;*Shh*^{GC}	89	0	0
Eed$^{+/+}$;*Ezh2*$^{+/-}$;*Shh*^{GC}	28	0	0
Eed$^{+/-}$;*Ezh2*$^{+/+}$;*Shh*^{GC}	62	7	11.3 (a)
Eed$^{+/-}$;*Ezh2*$^{+/-}$;*Shh*^{GC}	11	4	36.4 (b)
Eed$^{+/+}$;*Ezh2*$^{-/-}$;*Shh*^{GC}	19	10	52.6 (a)
Eed$^{-/-}$;*Ezh2*$^{+/+}$;*Shh*^{GC}	50	42	82 (a)
Eed$^{+/-}$;*Ezh2*$^{-/-}$;*Shh*^{GC}	13	3	77 (a)
Eed$^{-/-}$;*Ezh2*$^{+/-}$;*Shh*^{GC}	10	9	90 (a)
Eed$^{-/-}$;*Ezh2*$^{-/-}$;*Shh*^{GC}	5	5	100 (a)

a, P<0.05 vs wild type. b, P<0.05 vs the single heterozygous controls. Fisher's exact test.

Supplemental Table 2: qRT-PCR Primer Sequences for specific genes

Target Gene	Sequence 5' → 3'	Direction	Product Size
Ezh1	TCTTCCACGGCACCTATTTC TTCTGTGCAGGGTTCATGAG	Forward Reverse	147bp
Ezh2	TCCCGTTAAAGACCCTGAATG TGAAAGTGCCATCCTGATCC	Forward Reverse	149bp
Eed	TCCACTTTCCTGACTTTTCTACC CCATTTTGCCAGGTTTCCAG	Forward Reverse	128bp
p15	GAACCCTACCCAGTAAGACAAAG GCCCGGGAACTTCATACAATA	Forward Reverse	136bp
p16	CTTGGTCACTGTGAGGATTCA GATCCTCTCTAGCCTCAACAAC	Forward Reverse	142bp
Shh	ACGTAGCCGAGAAGACCCTA ACTTGTCTTTGCACCTCTGAGT	Forward Reverse	167bp
Ptch1	ACTGTCCAGCTACCCCAATG CATCATGCCAAAGAGCTCAA	Forward Reverse	198bp
Ptch2	GCGTACACCTCCCAGATGTT GGAACCCCTGATTTGTAGCA	Forward Reverse	172bp
Acta2	GTCCCAGACATCAGGGAGTAA TCGGATACTTCAGCGTCAGGA	Forward Reverse	102bp
Myh10	AGAAACACTGACCAAGCCTC ATCACATTCATCCCGAGCAG	Forward Reverse	77bp
Myh11	AAGCTGCGGCTAGAGGTCA CCCTCCCTTTGATGGCTGAG	Forward Reverse	219bp
MLCK	ACAAAAGCAGCTATGCCCCC TCCACCACCAGTGTGTAGCA	Forward Reverse	245bp
SM22a	CCAGACTGTTGACCTCTATGAAG TCTTATGCTCCTGGGCTTTC	Forward Reverse	145bp
Smtn	TCCTCTTCCTCGTCCTCGTC CTCTGTGCCTTCATTAACTCTTTC	Forward Reverse	136bp
Pax6	AGTGAATGGGCGGAGTTATG GAACTGACACTCCAGGTGAAA	Forward Reverse	122bp
Krt1	TCATCGACAAGGTGCGCTTC TGACTGGTCACTCTTCAGCG	Forward Reverse	170bp
Krt6a	AGTTGTTGGTACTCGGCGTT TTCGTGACCCTGAAGAAGGAT	Forward Reverse	132bp
Krt14	AGGAGACCAAAGGCCGTTAC GGTTGGTGGAGGTCACATCTC	Forward Reverse	276bp
Krt16	CAGTCCCAGCTCAGCATGAA TGTGAGGAGGAGCTGTGGATA	Forward Reverse	254bp
Krt17	TCCCAGCTCAGCATGAAAGC CTTGTACTGAGTCAGGTGGGC	Forward Reverse	252bp
Raldh2	AAGACACGAGCCCATTGGAG GGAAAGCCAGCCTCCTTGAT	Forward Reverse	180bp
Cyp26a1	CAGATGGTGCTTCAGCGGAG GAGGAATCGTGCAGGTTGGA	Forward Reverse	220bp
Cyp26b1	ATGCTGTTTGAAGGCTTGGAG AAGCCGGAACCCTGTAGCA	Forward Reverse	215bp
Foxa1	CAAGGATGCCTCTCCACACTT TGACCATGATGGCTCTCTGAA	Forward Reverse	114bp
PPARγ	ATTGAGTGCCGAGTCTGTGG GCCCAAACCTGATGGCATTG	Forward Reverse	226bp

Supplemental Table 3: Primer Sequences used in ChIP analysis

Target Gene	Sequence 5' → 3'	Direction	Product Size
p16	GTCCGATCCTTTAGCGCTGTT	Forward	71bp
	AGCCCGGACTACAGAAGAGATG	Reverse	
Pax6 (-12kb)	AAACTCTCAGGATTCGCGGG	Forward	155bp
	AAGGGAACGCGTTGGATAGG	Reverse	
Pax6 (-1.5kb)	CCAACCCAAAGGTACAACAGG	Forward	102bp
	GGTTTCCAAAGCATGGAGCC	Reverse	
Pax6 (-0.1kb)	CTAATCTGCCGAGCTGAACC	Forward	104bp
	GCAGGCGCTAACTTTCCTTA	Reverse	
Neg	ATTTTGTGCTGCATAACCTCCT	Forward	155bp
	TAGCAACATCCTAAGCTGGACA	Reverse	